J. Phys. Chem. C **2008,** *112,* 4925−4931

Silicon-Induced Strain Relaxation and Enhanced Gallium Surfactant Effects on Gallium Nitride Island Shaping

Z. L. Fang,*,† J. Y. Kang,† W. J. Huang,‡ H. T. Sun,§ M. Lu,§ J. F. Kong,∥ and W. Z. Shen∥

Semiconductor Photonics Research Center and Department of Physics, and Department of Chemistry, Xiamen University, Xiamen 361005, and Department of Optical Science and Engineering, Fudan University, Shanghai 200433, and Department of Physics, Shanghai Jiao Tong University, Shanghai 200030, People's Republic of China

Received: November 28, 2007; In Final Form: January 14, 2008

The self-organization of large-scale uniform aligned three-dimensional GaN nanoislands with triangular (0001) and distinct sidewall faceting has been realized by metal organic vapor-phase epitaxy on in situ Si-rich SiN_x nanoislands patterned c-sapphire substrates. We find that the GaN island shaping is closely related to the SiN_x pretreatment chemistry. It is suggested that enhanced surface Ga surfactant effects and compressive strain relaxation caused by site exchanges between excess Si and subsurface Ga atoms are responsible for the distinct triangular island shaping with large lateral size, smooth sidewall facets, and sharp triangle corners. Photoluminescence studies also show Si-doping-induced compressive strain relaxation and improved crystalline qualities for triangular GaN islands grown with the Si-rich SiN_x pretreatment.

I. Introduction

Self-organization of semiconductor nanostructures,[1−3] especially for GaN-based materials,[3−11] has attracted intense research interest due to the potential applications in nanoscale short-wavelength optoelectronic devices.[12−16] Syntheses of various GaN nanostructures have been realized by use of Stranski−Krastanov growth,[4] templates,[5−9] metal catalyst,[3,10,11] and surfactants/antisurfactants.[17] Recently, the self-organization of controlled nanocrystalline islands has become an important aspect of research due to the technological significance as well as the potential applications in fabrication of ordered arrays of nanoscale devices.[18−22] However, the uniformity in size and shape of coherent islands, which is a prerequisite for potential large-scale nanodevices applications, is difficult to obtain. For GaN heteroepitaxy, hexagonal pyramidal structures are generally formed under growth conditions of low temperature (LT) and high pressure due to the reduced adatom mobility (diffusion rates smaller than deposition rates).[23]

In this paper, we intentionally employ both excess Si and Ga as surfactants by purposefully in situ patterning of Si-rich SiN_x nanoislands on sapphire substrates and growth of GaN under Ga-rich conditions and successfully realize the self-organization of large-scale uniform aligned three-dimensional (3D) triangular nanocrystalline GaN islands. We find that the distinct triangular island shaping and drastic changes of island shape for GaN grown on substrates of different treatment processes are closely related to the treatment chemistry of the in situ SiN_x patterning. We attribute the phenomena to the Si-doping-induced compressive strain relaxation and the enhanced surface Ga surfactant effects.

* Corresponding author. E-mail: zhilaifang@hotmail.com.
† Semiconductor Photonics Research Center and Department of Physics, Xiamen University.
‡ Department of Chemistry, Xiamen University.
§ Fudan University.
∥ Shanghai Jiao Tong University.

II. Experimental Methods

The experiments were performed in a Thomas Swan metal organic chemical vapor deposition system. The c-plane sapphire substrates were thermally cleaned at 1060 °C and 100 Torr for 15 min under H_2 ambient followed by flowing 2500 sccm NH_3 at 545 °C for 4 min. After nitridation the SiN_x patterning was performed by introducing SiH_4 (100 ppm, 40 sccm) and NH_3 (2000 sccm) into the reactor simultaneously with H_2 as the carrier gas (5500 sccm).[24] Low-temperature growth with low NH_3/SiH_4 ratio and H_2 ambient was employed for patterning Si-rich SiN_x nanoislands on the substrate surface. On the in situ patterned substrate surface 25 nm GaN layers were grown at 535 °C and 500 Torr under Ga-rich growth conditions with trimethylgallium/NH_3/H_2 flow rates of 15/1700/7500 sccm.[25] During the annealing process,[26] the temperature was first ramped to 1035 °C in 400 s without changes of pressure and flow rates of NH_3/H_2. After the temperature reached 1035 °C, the reactor pressure was decreased to 300 Torr in 120 s with a H_2 flow rate of 6000 sccm. The surface morphologies of SiN_x layers and GaN layers were investigated by an atomic force microscope (AFM, PicoSPM and PSI XE-100) and a scanning electron microscope (SEM, LEO1530) equipped with an energy-dispersive X-ray spectrometer (EDX). The surface elemental information was characterized by X-ray photoelectron spectroscopy (XPS, PHI Quantum2000) and SEM−EDX. The photoluminescence (PL) excited by a 325 nm He−Cd laser was measured at low temperature (77 K) and room temperature (RT) for the GaN nucleation layers (NLs) prepared on sapphire substrates of different treatment methods.

III. Results and Discussion

Figure 1a shows a typical AFM image (5 μm × 5 μm) of “200 s LT SiN_x” pretreated substrate surface. In the figure the average island lateral size, island height, and island density are about 100 nm, 2 nm, and 1.4 × 10^9 cm^{-2}, respectively. Figure 1b shows that at the island sites Si was detectable, whereas at

10.1021/jp7112522 CCC: $40.75 © 2008 American Chemical Society
Published on Web 03/07/2008

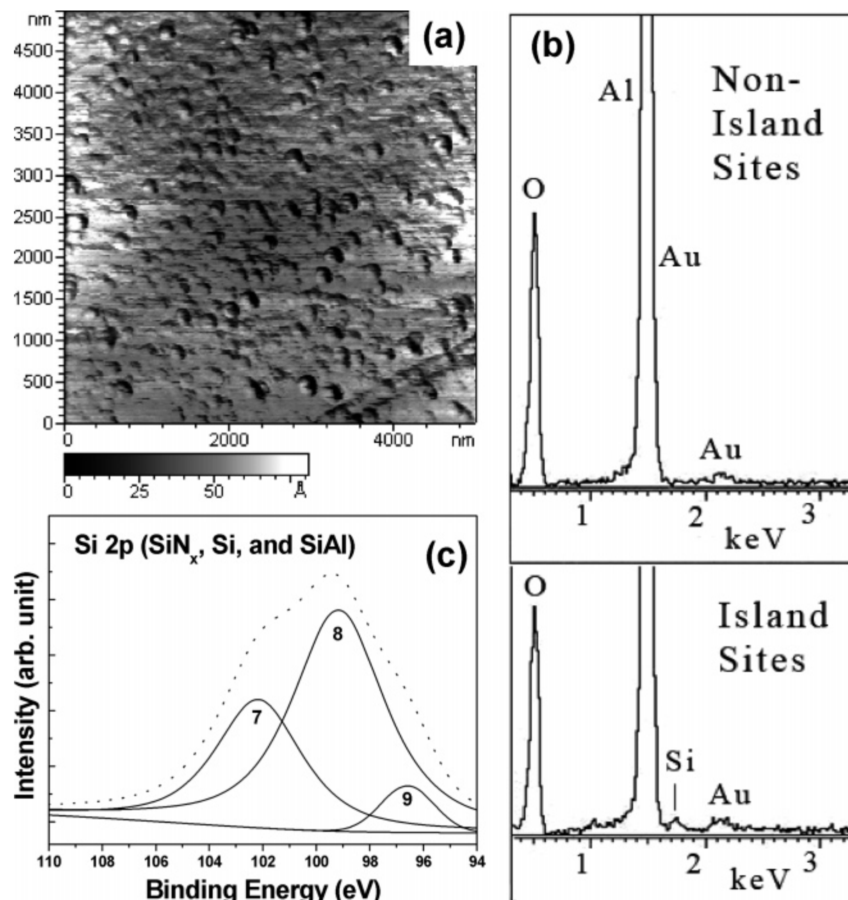

Figure 1. (a) Typical AFM image of the islandlike surface morphology (5 μm × 5 μm), (b) spatially resolved SEM−EDX analysis of surface composition, and (c) XPS spectra of the Si2p X-ray photoelectron peak of the "200 s LT SiN_x" layers predeposited on sapphire substrates. In the figure, the dotted curve is the Si2p X-ray photoelectron spectrum; the solid lines are the fitted peaks "7" (P7, 102.0 eV), "8" (P8, 99.3 eV), and "9" (P9, 96.5 eV) corresponding to Si2p (SiN_x), Si2p (Si), and Si2p (SiAl), respectively; "LT SiN_x" corresponds to SiN_x deposited at low temperature.

the nonisland sites Si was not detected. This implies that the sapphire surface was not fully covered by the SiN_x layer. Furthermore, the XPS spectrum of the Si2p photoelectron peak in Figure 1c confirms that the SiN_x layer was Si-rich with a Si/N ratio of about 3.2. The peak broadening of the X-ray photoelectron peaks was due to weak signals from the as-investigated nonstoichiometric SiN_x nanoislands not fully covering the sapphire substrates.

In Figure 2a we show a 10 μm × 10 μm AFM image for the surface morphology of annealed GaN layers grown on Si-rich SiN_x patterned substrate. A striking phenomenon of large-scale uniform aligned 3D islands of distinct triangular (0001) facets was observed. The line profile also shows that the islands are of island height of about 25 nm and have oblique sidewalls. The in-plane crystallographic alignment of the triangular base is in accordance with the (0001) sapphire substrate surface. The formation of triangular islands is due to the enhanced diffusion anisotropy.[27−29] By performing SEM−EDX measurements we found that Si was detected at the GaN island sites, whereas it was not detectable at the nonisland sites (Figure 2b). Furthermore, the island density of the GaN triangular islands is close to that of the SiN_x islands. Since SiN_x blocks GaN growth directly on the SiN_x islands, it is suggested that GaN preferentially nucleated on the bare sapphire surface surrounding the SiN_x islands followed by lateral overgrowth of GaN (∼25 nm) on the very thin SiN_x nanoislands (∼2 nm). This is actually an in situ nanoscale epitaxial lateral overgrowth method, in which the SiN_x nanoislands serve as the dielectric mask.

To further explore the effects of SiN_x on GaN island shaping, four types of GaN samples (A, B, C, and D) were prepared on substrates of different SiN_x treatment times and temperatures. All the other growth conditions for SiN_x and GaN remained the same as described above. For sample A there was no SiN_x patterning, i.e., GaN was grown on bare sapphire substrates. For samples B and C the SiN_x patterning was prepared at low temperature (545 °C) for 200 and 400 s, respectively. For sample D the SiN_x patterning was performed at high temperature (HT, 1035 °C) for 400 s. The SiN_x deposition at high temperature is expected to have more efficient dissociation of NH_3, and thus the SiN_x layers are expected to be less Si-rich. Typical AFM images for the surface morphologies of the four samples are shown in Figure 3. Islands of triangular base were observed for samples A−C. Without SiN_x treatment the triangular islands were nonuniform with rounded triangle corners (Figure 3a). With increase of the SiN_x treatment time to 200 s (Figure 3b) and 400 s (Figure 3c), the triangular GaN islands coarsened with a small reduction of island density from 2.4×10^9 to 1.3×10^9 and 7×10^8 cm^{-2}. The average side length of the triangles (estimated by one-third of the perimeter) is about 180, 240, and 330 nm, respectively. The change of island lateral size is consistent with that of island density for the same GaN deposition "thickness". As an example we show a typical line profile crossing the triangular islands (inset in Figure 3b) from which the angles of the oblique sidewall facets can be measured. When "LT SiN_x" treatment time increased from 0 to 400 s, the GaN islands became even sharper at the triangle corners. Corresponding to Figure 3 we show in Figure 4 the typical 3D

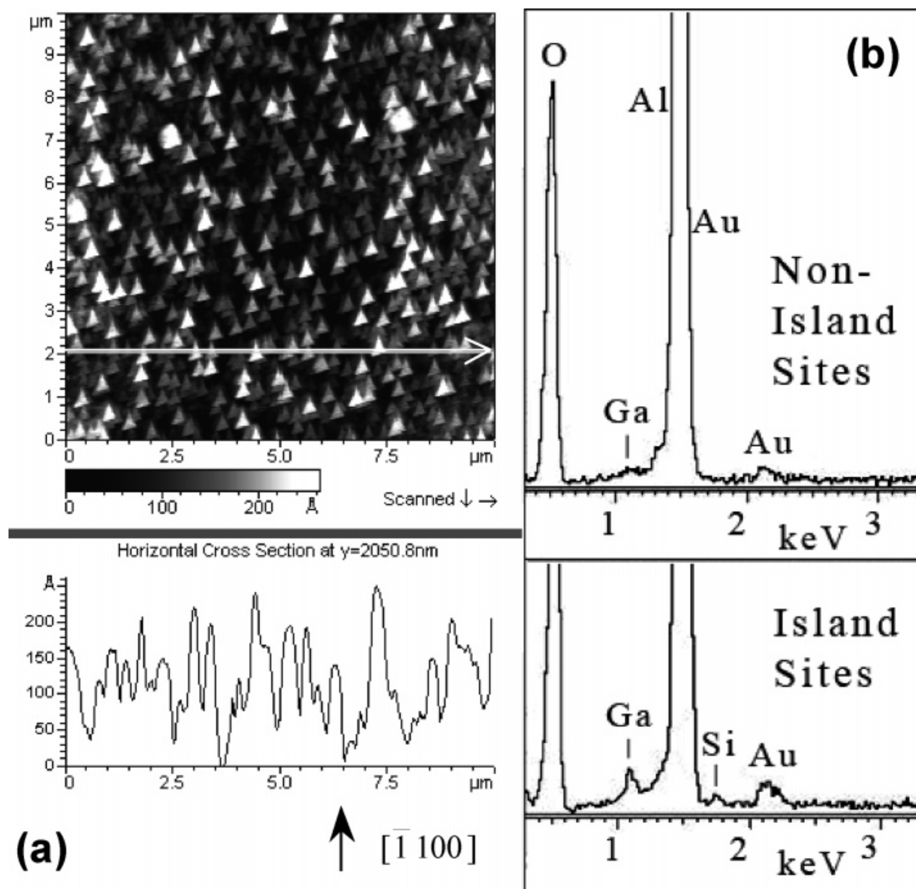

Figure 2. (a) Typical AFM image of the surface morphology (10 μm × 10 μm) of GaN layers grown on patterned sapphire substrates by Si-rich "LT SiN_x" nanoislands; a line profile crossing the islands over 10 μm is also shown. The crystallographic alignment of the triangular base is derived from the substrate. (b) SEM−EDX analysis showing Si detected at the GaN island sites, whereas it is not detected at the nonisland sites.

AFM images (1 μm × 1 μm) of the surface morphologies. Obviously, without SiN_x treatment the islands are domelike without distinct sidewall faceting (Figure 4a). With Si-rich SiN_x treatment the islands in Figure 4b are pyramid-like with triangular bases and sidewall faceting, and the triangular pyramids in Figure 4c have flat and wide top facets and very distinct sidewall faceting.

Considering the atomic radius of Ga, N, and Si (1.26, 0.75, and 1.10 Å), incorporation of Si at Ga substitutional sites (Si_{Ga}) is energetically favorable, whereas a large strain would be caused if Si is incorporated at the N sites (Si_N) or interstitial sites. Under Ga-rich growth conditions, Si prefers subsurface sites rather than surface sites, and thus the "kicked out" Ga atoms may form Ga bilayers on the surface, which is expected to reduce the Ehrlich−Schwoebel (ES) diffusion barrier.[29,30] Therefore, considering the critical island size proportional to the limited adatom diffusion length, the islands coarsened with the increase of SiN_x treatment time from 0 to 200 and 400 s; moreover, the reduction of the ES diffusion barrier has actually explained the reduction of island density because the formation of large islands by annihilation of very small islands becomes possible. Furthermore, the incorporation of Si into GaN relieves the compressive strain of GaN islands on sapphire and thus causes the variation of island shapes.[23,31] By measuring the oblique angle α of the sidewall facets referring to the (0001) plane (see the line profile in Figure 3b), we found that without SiN_x treatment the islands have steeper sidewalls of $\alpha_A \approx 24°$, whereas islands of samples B and C have $\alpha_B \approx 16°$ and $\alpha_C \approx 12°$, respectively. The increase of the critical lateral island size and the decrease of the oblique angle of the island sidewall facets for the triangular islands with the Si-rich "LT SiN_x" pretreatment have become an evidence for the Si-doping-induced strain relief and the enhanced surface Ga surfactant effect (in the following sections we will demonstrate the increase of "surface Ga" coverage when the Si-rich "LT SiN_x" pretreatment was employed).

To further study the chemistry of the SiN_x treatment process and the impact on island shaping, we prepared sample D grown under the same conditions as sample C except the deposition of SiN_x layers was at high temperature. The surface morphologies of sample D are shown in Figures 3d and 4d. It is interesting that hollow islands instead of triangular compact islands were observed. To understand the drastic changes of GaN island shapes, we investigated the chemistry of the SiN_x layers and GaN layers on substrates with different treatment methods.

Figure 5a shows the XPS spectrum of the Ga 3p photoelectron peak for GaN on sapphire substrates without SiN_x patterning and under Ga-rich growth conditions. According to the XPS data book,[32] the spectrum can be fitted into six peaks, P1 (109.2 eV), P2 (108.2 eV), P3 (107.2 eV), P4 (106.0 eV), P5 (105.0 eV), and P6 (104.0 eV), corresponding to Ga3p1/2 (Ga_2O_3), Ga3p1/2 (GaN), Ga3p1/2 (Ga), Ga3p3/2 (Ga_2O_3), Ga3p3/2(GaN), and Ga3p3/2 (Ga), respectively. The fitted peak areas of Ga3p3/2 were kept as twice that of Ga3p1/2. After annealing, Ga droplets are generally accumulated on bare substrates due to the high decomposition rate of GaN at high temperature and Ga-rich growth conditions. After exposure to air, surfaces of Ga are partially oxidized to form Ga_2O_3. We define $X^A_{Ga1/2} = (S^A_{P1} + S^A_{P3})/(S^A_{P1} + S^A_{P2} + S^A_{P3})$ and $X^A_{Ga3/2} = (S^A_{P4} + S^A_{P6})/$

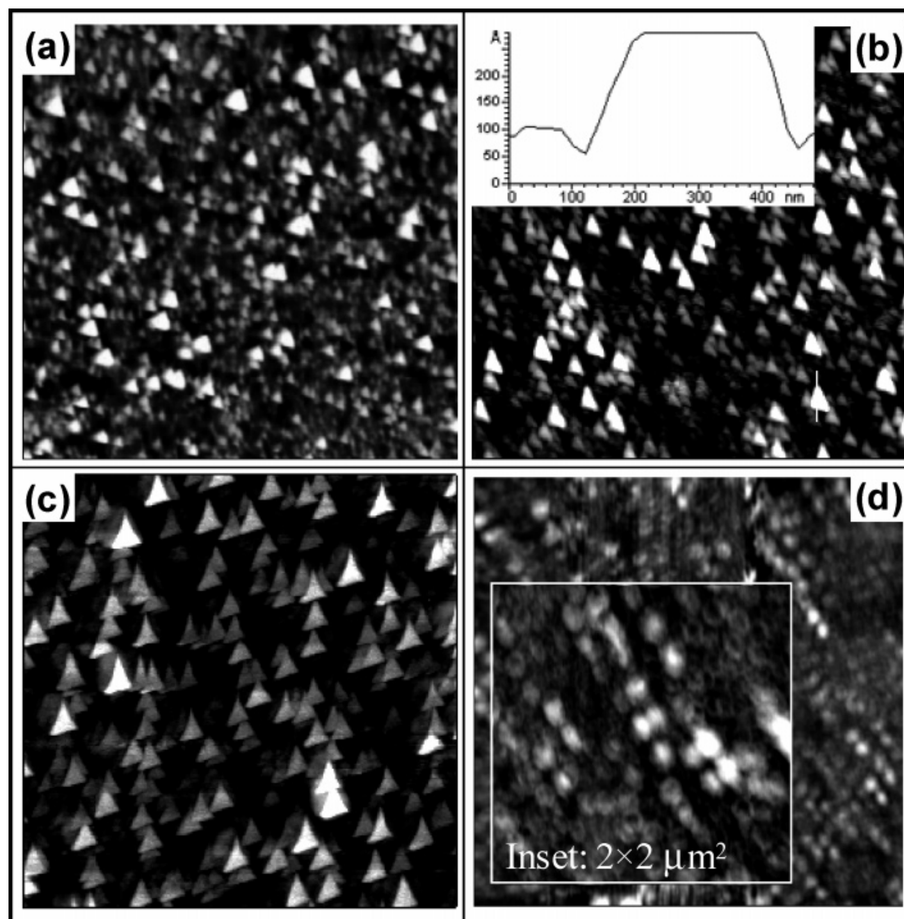

Figure 3. AFM image of the surface morphology of ∼25 nm GaN layers on (a) bare sapphire substrates, (b) "200 s LT SiN_x" treated substrates, (c) "400 s LT SiN_x" treated substrates, and (d) "400 s HT SiN_x" treated substrates, where HT denotes high temperature. The image size for (a−d) is 5 μm × 5 μm, and that for the inset in (d) is 2 μm × 2 μm. The inset in (b) is a line profile crossing a typical island, which clearly shows the oblique sidewall faceting.

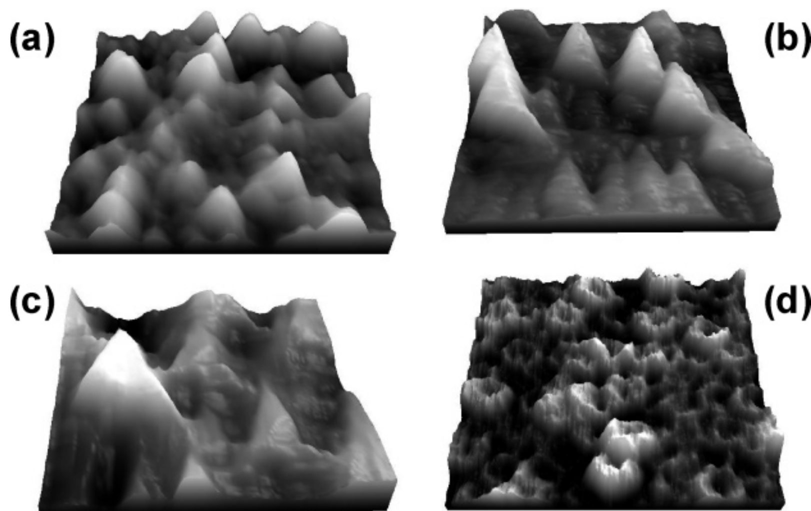

Figure 4. Three-dimensional AFM images of the surface morphology of 25 nm GaN layers on (a) bare sapphire substrates, (b) "200 s LT SiN_x" treated substrates, (c) "400 s LT SiN_x" treated substrates, and (d) "400 s HT SiN_x" treated substrates. The image size is 1 μm × 1 μm.

($S^A_{P4} + S^A_{P5} + S^A_{P6}$) here as a rough estimation for the coverage rate of "surface Ga" (including Ga droplets, adlayers, and oxidized Ga after exposure to air) in total Ga (including "surface Ga" and GaN) for the outermost surface layers of sample A, where S denotes the fitted peak area. We get $X^A_{Ga1/2} = X^A_{Ga3/2} = 47\%$. For comparison, in Figure 5b we show the XPS spectrum of the Ga3p photoelectron peak for a GaN sample prepared under much less Ga-rich growth conditions on sapphire substrates without SiN_x patterning. We find a decrease of the "surface Ga" coverage rate to $X^u_{Ga1/2} = X^u_{Ga3/2} = 40\%$. Therefore, employment of Ga-rich growth conditions could increase the "surface Ga" coverage rate.

Figure 5c shows the XPS spectra (Ga3p and Si2p) of GaN grown on substrates with SiN_x pretreatment for 400 s at low temperature. In comparison with Figure 5, parts a and b, a small and broad new peak P7 (102.0 eV) corresponding to Si2p (SiN_x)

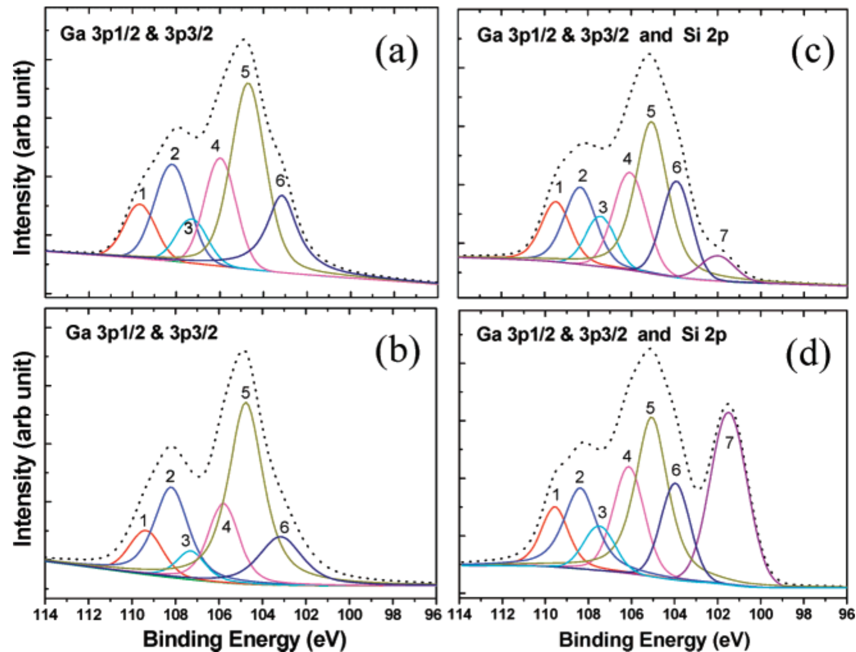

Figure 5. XPS spectra of the Si2p and Ga3p photoelectron peaks of ~25 nm GaN layers on (a) bare sapphire substrates under Ga-rich growth conditions, (b) bare sapphire substrates under much less Ga-rich growth conditions, (c) "400 s LT SiN_x" treated substrates, and (d) "400 s HT SiN_x" treated substrates. In the figure, the dotted curve is the Ga3p and Si2p X-ray photoelectron spectrum; the solid lines are the fitted peaks "1" (P1, 109.2 eV), "2" (P2, 108.2 eV), "3" (P3, 107.2 eV), "4" (P4, 106.0 eV), "5" (P5, 105.0 eV), "6" (P6, 104.0 eV), and "7" (P7, 102.0 eV) corresponding to Ga3p1/2 (Ga_2O_3), Ga3p1/2 (GaN), Ga3p1/2 (Ga), Ga3p3/2 (Ga_2O_3), Ga3p3/2 (GaN), Ga3p3/2 (Ga), and Si2p (SiN_x), respectively.

appears because of the Si-rich SiN_x pretreatment. The "surface Ga" coverage rate increased to $X^{C}_{Ga1/2} = X^{C}_{Ga3/2} = 57\%$. This has become an experimental evidence that the presence of excess Si in Si-rich SiN_x islands would induce the Si−Ga exchange process and thus further increase the "surface Ga" coverage rate, i.e., $X^{C}_{Ga} > X^{A}_{Ga} > X^{u}_{Ga}$. The increase of surface Ga coverage reduces the ES diffusion barrier and thus increases the critical diffusion length and critical island size (Ga surfactant effect). Furthermore, the island edge adatoms would have higher probability to migrate and reach the triangle corners; hence, sharp triangle corners were formed (Figure 3c).

Figure 5d shows the XPS spectra (Ga3p and Si2p) of GaN grown on substrates with SiN_x pretreatment for 400 s at high temperature. For HT SiN_x treatment the intensity of P7 became very strong. This is consistent with the XPS spectrum of the Si2p photoelectron peak of SiN_x layers deposited at high temperature (Figure 6). The formation of thick SiN_x layers is due to the high dissociation efficiency of NH_3 and deposition rate of SiN_x at high temperature. Meanwhile, in Figure 6 peaks P8 (99.3 eV) and P9 (96.5 eV) corresponding to Si and SiAl alloy are very weak and broad compared with peak P7. This has indicated that the HT-prepared SiN_x islands were not Si-rich (Si/N ≈ 1) as compared to the LT-prepared SiN_x islands as shown in Figure 1c. The deficiency of Si in the SiN_x islands lowered the Si−Ga exchange rate. This has been evidenced by Figure 5d in which the "surface Ga" coverage rate is estimated to be $X^{D}_{Ga1/2} = X^{D}_{Ga3/2} = 49\%$. As a result, the adatom mobility would be decreased compared with that of sample C. The decrease of adatom mobility increased the GaN nucleation rates at the SiN_x island edges so that the SiN_x islands could be circled by the GaN islands as the bounding wall. Furthermore, due to the limited diffusion length (<20 nm for Ga adatoms), no distinct triangular GaN islands were formed. Further growth of GaN at high temperature resulted in the formation of large islands of hexagonal bases and sidewall facets due to the gas-phase transport dominating growth mechanism and the limited

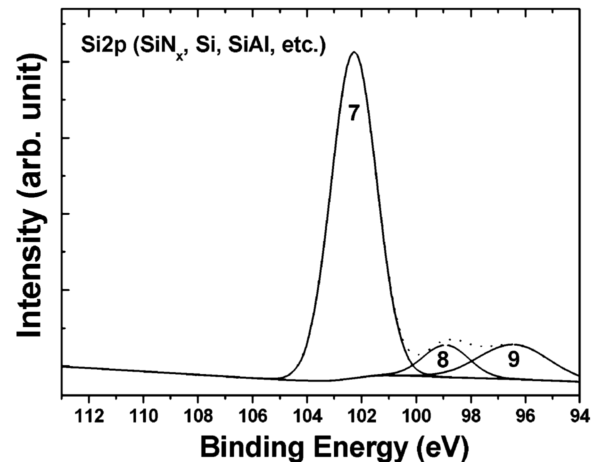

Figure 6. XPS spectra of the Si2p photoelectron peak of the "400 s HT SiN_x layers" on sapphire substrates. In the figure, the dotted curve is the Si2p X-ray photoelectron spectrum; the fitted peaks "7" (P7, 102.0 eV), "8" (P8, 99.3 eV), and "9" (P9, 96.5 eV) correspond to Si2p (SiN_x), Si2p (Si), and Si2p (SiAl), respectively.

diffusion length of edge adatoms compared with the increased island size.[29,33]

The RT PL of samples A, C, and D have also been measured and are shown in Figure 7. At RT the near band edge emissions are broad with a long tail of UV luminescence (UVL) possibly arisen from the surface structural defects and interface states.[33] In comparison with samples A (without SiN_x treatment) and D (with non-Si-rich "400 s HT SiN_x" treatment), a red shift of the GaN near band edge emission was observed for sample C (with Si-rich "400 s LT SiN_x" treatment), which suggested Si-induced compressive strain relaxation of GaN on sapphire and luminescence from the distinct sidewall facets.[31,35] For further comparisons we also measured the LT PL of samples A, C, and D at 77 K. Clearly, as shown in Figure 8, the intensity peak of the band edge emission (hexagonal GaN) of the triangular GaN islands on Si-rich "400 s LT SiN_x" treated

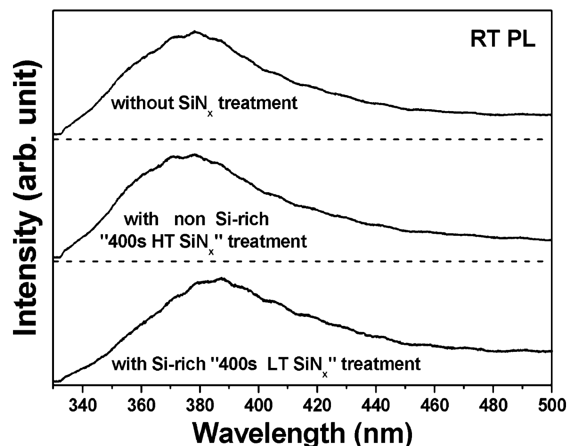

Figure 7. Room-temperature photoluminescence (RT PL) of GaN islands on bare sapphire substrates and “400 s HT SiN_x” and “400 s LT SiN_x” treated substrates.

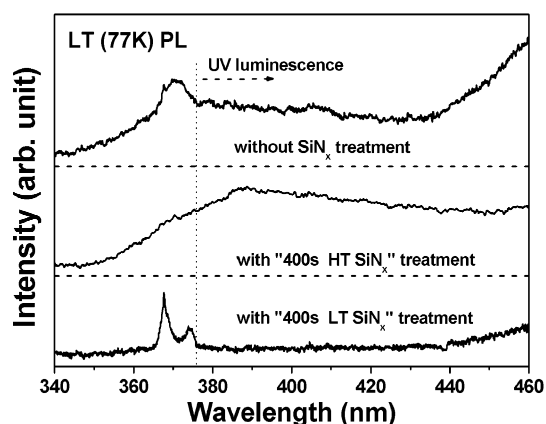

Figure 8. Low-temperature (77 K) photoluminescence (LT PL) of GaN islands on bare sapphire substrates and “400 s HT SiN_x” and “400 s LT SiN_x” treated substrates.

substrates is much sharper than that of GaN islands on bare sapphire substrates and on “400 s HT SiN_x” treated substrates. The improved crystalline quality and distinct sidewall faceting of the triangular GaN islands on the Si-rich “400 s LT SiN_x” treated substrate are likely responsible for the sharpness of the band edge emission lines. The UVL (starting from 375 nm), related to the excitons bound to surface structural defects and interface states, and the donor bound excitons (DBE) of cubic GaN (379 nm) are almost invisible for the distinct triangular GaN islands (sample C) compared with that of the conventional LT GaN NLs (the nucleated islands of indistinct shapes, e.g., sample A) and that of GaN islands on “400 s HT SiN_x” treated sapphire (sample D);[34] in comparison with samples A and D, the reduction of UVL intensity for sample C indicates better strain relaxation and crystalline qualities; the disappearance of the DBE (cubic GaN) peak for LT GaN NLs with Si-rich SiN_x treatment seems to imply a more efficient transition from cubic to hexagonal during the annealing process; hence, we infer that better crystalline quality and strain relief have been obtained for the triangular GaN nanoislands prepared on the Si-rich “400 s LT SiN_x” treated sapphire substrates. The identification of all the luminescence lines remains not clear yet.[34] Further detailed luminescence studies on a set of LT GaN NLs (nucleated islands) prepared under various growth conditions are needed.

IV. Conclusion

In summary, we have realized the self-organization of large-scale uniform aligned 3D GaN islands of triangular (0001) and distinct sidewall faceting by means of in situ thin Si-rich “LT SiN_x” nanoislands patterning on the c-sapphire substrates and growth of GaN under Ga-rich conditions. We find that the in situ pretreatment chemistry of SiN_x on sapphire substrates has significant influences on the GaN island shaping. The increase of “surface Ga” coverage rate caused by the Si−Ga site exchange and thus enhanced surface Ga surfactant effect resulted in the formation of GaN nanoislands with larger lateral size, smoother sidewall facets, and sharper triangle corners when the “LT SiN_x” treatment time increased from 0 to 200 and 400 s. In addition to the surface Ga surfactant effect, intentional Si-doping via patterning of Si-rich SiN_x nanoislands also relieved the compressive strain of GaN on sapphire and caused the variation of island shapes. Strain relaxation and enhanced surface Ga surfactant effects are responsible for the remarkable uniformity and distinct shaping of the strained islands. Photoluminescence studies showed Si-doping-induced compressive strain relaxation of GaN on sapphire and improved crystalline qualities for distinct triangular GaN islands on Si-rich “LT SiN_x” treated sapphire. Further studies on optimization of the growth conditions of SiN_x and GaN nanoislands for better regularity and crystalline qualities, the optical properties, and applications will be continued.

Acknowledgment. This work was partially supported by the “863” program, National Natural Science Foundation of China, and Fujian key Laboratory of Semiconductors and Applications.

Supporting Information Available: SEM and PL data of larger GaN islands of quasi-hexagonal and hexagonal base. This material is available free of charge via the Internet at http://pubs.acs.org.

References and Notes

(1) Teichert, C. *Phys. Rep.* **2002**, *365*, 335.
(2) Xia, Y. N.; Yang, P. D. *Adv. Mater.* **2003**, *15*, 351.
(3) Kuykendall, T.; Pauzauskie, P.; Lee, S. K.; Zhang, Y. F.; Goldberger, J.; Yang, P. D. *Nano Lett.* **2003**, *3*, 1063.
(4) Brown, J.; Wu, F.; Petroff, P. M.; Speck, J. S. *Appl. Phys. Lett.* **2004**, *84*, 690.
(5) Goldberger, J.; He, R. R.; Zhang, Y. F.; Lee, S. W.; Yan, H. Q.; Choi, H. J.; Yang, P. D. *Nature* **2003**, *422*, 599.
(6) Chen, P.; Chua, S. J.; Tan, J. N. *Appl. Phys. Lett.* **2006**, *89*, 23114.
(7) Kuykendall, T.; Pauzauskie, P. J.; Zhang, Y. F.; Goldberger, J.; Sirbuly, D.; Denlinger, J.; Yang, P. D. *Nat. Mater.* **2004**, *3*, 524.
(8) Deb, P.; Kim, H.; Rawat, V.; Oliver, M.; Kim, S.; Marshall, M.; Stach, E.; Sands, T. *Nano Lett.* **2005**, *5*, 1847.
(9) Hersee, S. D.; Sun, X.; Wang, X. *Nano Lett.* **2006**, *6*, 1808.
(10) Su, J.; Cui, G.; Gherasimova, M.; Tsukamoto, H.; Han, J.; Ciuparu, D.; Lim, S.; Pfefferle, L.; He, Y.; Nurmikko, A. V.; Broadbridge, C.; Lehman, A. *Appl. Phys. Lett.* **2005**, *86*, 13105.
(11) Xu, B. S.; Yang, D.; Wang, F.; Liang, J.; Ma, S. F.; Liu, X. G. *Appl. Phys. Lett.* **2006**, *89*, 74106.
(12) Huang, Y.; Duan, X.; Cui, Y.; Lieber, C. M. *Nano Lett.* **2002**, *2*, 101.
(13) Qian, F.; Li, Y.; Gradecak, S.; Wang, D. L.; Barrelet, C. J.; Lieber, C. M. *Nano Lett.* **2004**, *4*, 1975.
(14) Zhong, Z. H.; Qian, F.; Wang, D. L.; Lieber, C. M. *Nano Lett.* **2003**, *3*, 343.
(15) Kim, H. M.; Kang, T. W.; Chung, K. S. *Adv. Mater.* **2003**, *15*, 567.
(16) Johnson, J. C.; Choi, H. J.; Knutsen, K. P.; Schaller, R. D.; Yang, P. D.; Saykally, R. J. *Nat. Mater.* **2002**, *1*, 106.
(17) Neugebauer, J. *Phys. Status Solidi C* **2003**, *0*, 1651.
(18) Kodambaka, S.; Khare, S. V.; Petrov, I.; Greene, J. E. *Surf. Sci. Rep.* **2006**, *60*, 55.
(19) Evans, J. W.; Thiel, P. A.; Bartelt, M. C. *Surf. Sci. Rep.* **2006**, *61*, 1.
(20) Deng, X.; Weil, J. D.; Krishnamurthy, M. *Phys. Rev. Lett.* **1998**, *80*, 4721.
(21) Sutter, P.; Lagally, M. G. *Phys. Rev. Lett.* **1998**, *81*, 3471.
(22) Wang, L. G.; Kratzer, P.; Scheffler, M.; Moll, N. *Phys. Rev. Lett.* **1999**, *82*, 4042.

(23) Shahedipour-Sandvik, F.; Grandusky, J.; Alizadeh, A.; Keimel, C.; Ganti, S. P.; Taylor, S. T.; LeBoeuf, S. F.; Sharma, P. *Appl. Phys. Lett.* **2005**, *87*, 233108.

(24) (a) Haffouz, S.; Lahreche, H.; Vennegues, P.; de Mierry, P.; Beaumont, B.; Omnes, F.; Gibart, P. *Appl. Phys. Lett.* **1998**, *73*, 1278. (b) Haffouz, S.; Kirilyuk, V.; Hageman, P. R.; Macht, L.; Weyher, J. L.; Larsen, P. K. *Appl. Phys. Lett.* **2001**, *79*, 2390. (c) Fang, Z. L.; Li, S. P.; Li, J. C.; Sun, H. Z.; Wang, S. J.; Kang, J. Y. *Thin Solid Films*, in press, doi:10.1016/j.tsf.2007.12.132.

(25) Amano, H.; Sawaki, N.; Akasaki, I.; Toyoda, Y. *Appl. Phys. Lett.* **1986**, *48*, 353.

(26) Lada, M.; Cullis, A. G.; Parbrook, P. J. *J. Cryst. Growth* **2003**, *258*, 89.

(27) Xie, M. H.; Gong, M.; Pang, E. K. Y.; Wu, H. S.; Tong, S. Y. *Phys. Rev. B* **2006**, *74*, 085314.

(28) Zhang, Z.; Chen, X.; Lagally, M. G. *Phys. Rev. Lett.* **1994**, *73*, 1829.

(29) Fang, Z. L.; Kang, J. Y. *J. Phys. Chem. C* **2007**, *111*, 7889.

(30) Rosa, A. L.; Neugebauer, J. *Phys. Rev. B* **2006**, *73*, 205314.

(31) Lee, I. H.; Choi, I. H.; Lee, C. R.; Noh, S. K. *Appl. Phys. Lett.* **1997**, *71*, 1359.

(32) Moulder, J. F.; Stickle, W. F.; Sobol, P. E.; Bomben, K. D. *Handbook of X-ray Photoelectron Spectroscopy: A Reference Book of Standard Spectra for Identification and Interpretation of XPS Data*; Physical Electronics: Minnesota, 1995.

(33) See the Supporting Information.

(34) Reshchikov, M. A.; Morkoç, H. *J. Appl. Phys.* **2005**, *97*, 061301.

(35) Li, X.; Bohn, P. W.; Kim, J.; White, J. O.; Coleman, J. J. *Appl. Phys. Lett.* **2000**, *76*, 3031.